Imino Proton Exchange in DNA Catalyzed by Ammonia and Trimethylamine: Evidence for a Secondary Long-Lived Open State of the Base Pair†

Sebastian Wärmländer, Anjana Sen, and Mikael Leijon*

Department of Biophysics, Arrhenius Laboratory, Stockholm University, S-106 91 Stockholm, Sweden

Received August 10, 1999; Revised Manuscript Received October 15, 1999

ABSTRACT: The base-pair opening kinetics of the self-complementary oligomer d(CGCGAATTCGCG)$_2$ has been derived from NMR measurements of the imino proton exchange. In general, it has previously been found that imino proton exchange in duplex DNA is limited by the proton-transfer step from the open state and that the dependence of the exchange times on the inverse concentration of an added exchange catalyst is linear. In the present study, a curvature is observed for, in particular, the innermost AT base pair with both ammonia and trimethylamine (TMA) as exchange catalysts. The two catalysts act on the same open states, but the accessibility of TMA is reduced by a factor of 2−3 compared to ammonia. Assuming that ammonia accesses the imino proton equally in the open state of the base pair and in the mononucleoside, the curvature is consistent with 7−9% of the openings ending in open states with lifetimes of about 1 μs while the bulk of open-state lifetimes fall in the nanosecond range. A curvature is also found for the exchange times of the imino protons in the A-tract sequence CGCA$_8$CGC/GCGT$_8$GCG. This curvature becomes increasingly pronounced from the 5′-end toward the center of the tract and hereby seems to be correlated with the contraction of the minor groove. Thus, while the base-pair lifetimes deduced from the present study are in accordance with previous measurements, a substantial fraction of the open states formed by the central AT-base pairs in the two oligomers exhibits microsecond lifetimes in contrast to previous estimates in the nanosecond range. These findings may be of relevance for the way sequence specific recognition is accomplished by proteins and ligands.

Base-pair opening in double-stranded DNA is important in cellular processes such as DNA transcription and recombination. In addition, the dynamics of base-pair opening has been shown to reflect sequence dependent properties of the DNA double helix, such as groove width and flexibility (*1*). The ability of a DNA sequence element to adjust the structure in order to achieve favorable intermolecular contacts in protein−DNA complexes is important in recognition (*2*−*4*) and may have a counterpart in base-pair dynamics. For instance, the target cytosine of the M.*Hha*I[1] and M.*Hae*III cytosine-5 methyltransferases are completely flipped out from the helix in the complexes between the recognition sequences and the enzymes (*5*, *6*). Consequently, base-pair opening is a critical step in the enzymatic mechanism. Subsequently, it was found that tracts of several consecutive GC base pairs, of the type found in the recognition sequences of Cytosine-5 methyltransferases, exhibit an unexpectedly rapid base-pair dynamics (*7*). Hence, the propensity of the recognition sequence to adopt the structure imposed in the DNA−protein complex may contribute to the specificity of M·*Hha*I and M·*Hae*III. Furthermore, information regarding base-pair opening is also important to understand the factors that govern the stability of nucleic acid structures. For these reasons, the base-pair opening process in double-helical DNA has been the subject of intensive investigation (*1*, *8*).

The imino protons exchange with the solvent protons only when the hydrogen bond in the base pair is disrupted (*8*, *9*). The chemical proton-transfer step from the open state is usually rate limiting, and a proton acceptor must be added to accelerate the exchange close to opening-limited conditions. The base-pair lifetimes are obtained by extrapolation of the exchange times to infinite catalyst concentration (*10*−*12*). The dissociation constant of a base pair can be estimated by comparing the exchange rates of the imino proton in the base pair and in the mononucleoside. The unknown factor in this comparison is the accessibility of the imino proton in the open base pair, which is related to properties of the open state. It has been suggested that information about the nature of the open state could be obtained from distinctive catalytic properties of different catalysts (*13*). Measurements of the solvent exchange by utilizing its effect on the NMR relaxation rates of the imino protons have yielded lifetimes in the range 1−40 ms for base pairs in B-DNA (*1*). However, the sequence composition (*7*, *14*), the charged state of the double helix (*15*), and drug interactions (*16*, *17*) modulate base-pair dynamics strongly.

The present work investigates the properties of the open state in double helical DNA utilizing imino proton exchange catalysts with different size, and further examines our recent observation that exchange catalysis by TMA yields longer base-pair lifetimes than by ammonia (*15*). As a suitable

† This work was supported by the Swedish Natural Science Research Council, the Magnus Bergvall Foundation, the Lars Hierta Memorial Foundation and the Harald Jeansson Foundation.

* To whom correspondence should be addressed. Phone: (+46)-8-16 24 47. Fax: (+46)-8-15 55 97. E-mail: leijon@biophys.su.se.

[1] Abbreviations: CD, circular dichroism; FID, free induction decay; M.*Hha*I and M.*Hae*III, methyltransferases; NMR, nuclear magnetic resonance; PNA, peptide nucleic acid; TMA, trimethylamine.

10.1021/bi991863b CCC: $19.00
Published on Web 12/23/1999

Chart 1: Base Pair Numberings

```
   1 2 3 4 5 6 6 5 4 3 2 1
5'-C G C G A A T T C G C G-3'
3'-G C G C T T A A G C G C-5'

   1 2 3 4 5 6 7 8 9 10 11 12 13 14
5'-C G C A A A A A A A A C G C-3'
3'-G C G T T T T T T T T G C G-5'
```

model system, the self-complementary 12-mer d(CGCGAATTCGCG)$_2$ was chosen. The base-pair kinetics of this oligomer have been extensively investigated [see Guéron and Leroy (*12*), for a review]. In addition, the 14-mer CGCA$_8$CGC/GCGT$_8$GCG with an eight base-pair A-tract core was studied. The base-pair numberings used in the text are shown in Chart 1.

We find that at high concentrations of the two catalysts the exchange times converge to the same extrapolated base-pair lifetimes. Although, to the best of our knowledge, all previous investigations of imino proton exchange in double helical nucleic acids have found that Linderstrøm-Lang kinetics (*18*) is obeyed and that the exchange times display a linear dependence on the inverse base catalyst concentration (*12*), we observe nonlinear τ_{ex} vs 1/[B] plots for the central AT base pair of d(CGCGAATTCGCG)$_2$. Comparison of the exchange catalysis by TMA and ammonia at different temperatures indicates the existence of a secondary open state with almost 2 orders of magnitude longer lifetimes than previously identified open states. The exchange times for the thymine imino protons in the A-tract sequence CGCA$_8$CGC/GCGT$_8$GCG show an even more pronounced curvature that increases toward the center of the tract. These observations are discussed in regard to the process of base-pair opening and the properties of the open states in double helix DNA.

MATERIALS AND METHODS

Sample Preparation and Titrations. The oligonucleotides d(CGCGAATTCGCG)$_2$ and CGCA$_8$CGC/GCGT$_8$GCG were purified twice on NAP 10 Columns, dissolved in a 3 mM borate buffer containing 100 mM NaCl, and adjusted to appropriate pH. The duplex concentrations were in the range 0.5−3 mM.

The 12-mer was titrated with five different buffers: a 6.6 M ammonia buffer at pH 9.5, a 4.3 M TMA buffer at pH 9.5, a 6.3 M ammonia buffer at pH 8.8, a 5.5 M ammonium chloride salt solution at pH 4.6, and a 4.3 M trimethylammonium chloride salt solution at pH 6.0. The 14-mer was titrated with the 6.3 M ammonia buffer at pH 8.8, and the 5.5 M ammonium chloride salt solution at pH 4.6. The pH values of the buffers were measured with a double-junction high-salt Orion 8103 Ross electrode. Calculations based on ionic mobilities using the Henderson equation (*19*) indicated that the liquid junction potential in the pH electrode, introduced by the high-salt concentrations used, produced an error less than 0.1 pH units. Because of activity effects, the Henderson−Hasselbalch equation does not give correct [acid]/[base] fractions of the buffers. These fractions were instead simply obtained from the amounts of salt and liquid base used to prepare the buffers.

The mononucleosides, thymidine and 2′-deoxyguanosine, were dissolved in water to a concentration of 5.0 mM. The pH was titrated from 6.5 to 3.5 by small additions of HCl, both in the absence and in the presence of 8.6 mM ammonia or TMA buffer. The pH was measured directly in the NMR tube with an Orion 9826 Micro-pH Electrode. The NMR tube was immersed in a thermostatically controlled waterbath maintained at 20 °C during the pH measurements. The pH before and after each NMR experiment was found to vary by no more than ±0.05 units. The Henderson−Hasselbalch equation was used to calculate the base fraction of the catalyst at each pH using pK_a values of 9.35 and 9.87 for ammonia and TMA, respectively (*20*).

Imino Proton Exchange Theory. The imino proton-transfer rate from the mononucleoside per mole of catalyst k_{tr}^i is related to the molar collision rate k_{coll} and the pK_a difference between the imino proton and the catalyst $\Delta pK = pK_{a,I} - pK_{a,B}$ by (*21*)

$$k_{tr}^i = \frac{k_{coll}}{1 + 10^{\Delta pK}} \tag{1}$$

Since the solution pH used in the NMR measurements on the mononucleosides is far below the pK_a of both buffers, the base catalyst concentration is given by the fraction $10^{pH-pK_{a,B}}$ of the total buffer concentration [T]. The imino proton exchange rate $k_{ex}^i = [B]k_{tr}^i$ is then related to the solution pH by

$$\log\left(\frac{1}{k_{ex}^i}\right) = pK_{a,B} + \log\left(\frac{1}{k_{tr}^i[T]}\right) - pH \tag{2}$$

Hence, for a given buffer concentration, a plot of $\log(1/k_{ex}^i)$ vs pH affords a straight line with slope 1 from which the intrinsic transfer rate k_{tr}^i can be obtained.

It is generally considered that exchange of the imino proton in the base pair only occur from an open state where the imino proton lacks hydrogen bonding (*8*). For a base pair with multiple open states, formed with rates k_{op}^n and closed with rates k_{cl}^n, and provided that $\sum_n k_{op}^n \ll k_{cl}^1, k_{cl}^2, ..., k_{cl}^m$, the total imino proton exchange rate k_{ex} equals the sum of the exchange rate from each mode:

$$k_{ex} = \sum_{n=1}^{m} \frac{k_{op}^n k_{tr}^i[B]}{k_{cl}^n/\alpha^n + k_{tr}^i[B]} \tag{3}$$

where k_{tr}^i is, as above, the intrinsic imino proton-transfer rate from the mononucleoside and α^n is a parameter taking into account the different accessibility of the imino proton in the open states and in the mononucleoside. For a base pair with a single opening mode ($n = 1$) and with $k_{op} \ll k_{cl}$, eq 3 can be rewritten as

$$\tau_{ex} = \tau_{op} + \frac{1}{K_d \alpha k_{tr}^i[B]} \tag{4}$$

where τ_{ex} and τ_{op} are the inverse exchange and opening rate, respectively, and $K_d = k_{op}/k_{cl}$ is the base pair dissociation constant. If eq 4 is valid, a plot of τ_{ex} versus 1/[B] yields a straight line where τ_{op} is obtained from the *y*-axis intercept and αK_d from the slope. The limit where eq 4 is valid will be referred to as Linderstrøm−Lang kinetics (*18*).

Imino Proton Resonance Assignments. The imino proton resonance assignment of the 12-mer has been published (*22*).

For assignment of the 14-mer, a NOESY experiment with a mixing time of 250 ms was acquired at 20 °C on a Varian Inova 600 MHz spectrometer. A Jump-Return observe pulse was used to avoid excitation of the solvent resonance (*23*). Linear prediction was employed in the indirect dimension to increase resolution close to the diagonal. All 2D data processing were carried out with Felix97 (Molecular Simulations Inc.). From imino−imino connectivities, it was clear that the imino proton resonances in the A-tract shift progressively either upfield or downfield from one end of the tract to the other. By comparison of assignments in closely similar sequences (*24*), the direction of the tract could be established.

Exchange Measurements. The NMR experiments on the duplexes and the mononucleosides were carried out on a Varian Inova 600 and 400 MHz spectrometer, respectively. The imino proton exchange times τ_{ex} at different catalyst concentrations were obtained from measurements of the inversion recovery times in the presence (T_{rec}) and in absence (T_{aac}) of exchange catalyst according to

$$\frac{1}{\tau_{ex}} = \frac{1}{T_{rec}} - \frac{1}{T_{aac}} \quad (5)$$

Except longitudinal dipolar relaxation, direct exchange to water as well as exchange catalyzed by OH^--ions and the acceptor nitrogen of the opposite base (*25*) contributes to the recovery rate of the imino protons in the absence of added catalyst $1/T_{aac}$. However, these contributions remain constant when the catalyst is added and will be canceled in eq 5. Consequently, the exchange time τ_{ex} represents exchange only via the added catalyst.

The inversion recovery experiment utilized a 1−1.4 ms iBURP pulse for selective inversion (*26*) and a 0.7−1 ms Gaussian observe pulse (*27*). Right shift and linear prediction of the FID were employed to correct for magnetization evolution during the observe pulse. For the mononucleosides, exchange times were also obtained from the line widths of the imino proton resonances in the presence (ν_{cat}) and in absence (ν_{aac}) of exchange catalyst according to

$$\tau_{ex} = \frac{1}{\pi(\upsilon_{cat} - \upsilon_{aac})} \quad (6)$$

Line widths were measured in spectra acquired with a Jump-Return observe pulse (*23*).

CD Spectroscopy. CD spectra of $d(CGCGAATTCGCG)_2$ were recorded in the interval 240−320 nm at 20 °C on a Jasco-720 spectropolarimeter equipped with a thermoelectrically controlled cell holder using 500 μL cuvettes with 1 cm path length. The spectra were collected as the average of 10 scans. The oligomer was dissolved in a solution containing 0.1 M NaCl or, additionally, either ammonia or TMA buffer added to 2.9 and 2.2 M concentrations, respectively. In all solutions, the pH was adjusted to 9.5. The duplex concentration was 10 μM.

Activation Parameters for Base-Pair Opening. The Gibbs' free energy of activation for the base-pair opening $\Delta G^{‡\circ} = \Delta H^{‡\circ} - T\Delta S^{‡\circ}$ is obtained from the opening rates k_{op} measured at different temperatures by application of the Eyring equation (*28*):

$$\ln(k_{op}/T) = \ln(\kappa k/h) - \Delta H^{‡\circ}/RT + \Delta S^{‡\circ}/R \quad (7)$$

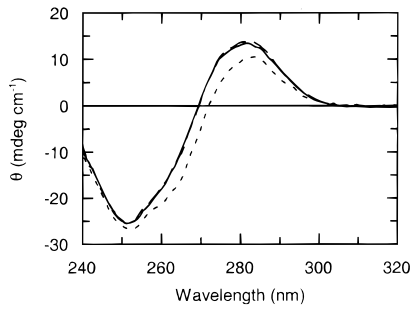

FIGURE 1: (a) CD spectrum of $d(CGCGAATTCGCG)_2$ at 20 °C and in a 3 mM borate buffer at pH 9.5 in the presence of either (—) 0.1 M NaCl, (- - -) 2.9 M ammonia, or (— — —) 2.2 M TMA buffer.

where $\Delta H^{‡\circ}$ and $\Delta S^{‡\circ}$ are the activation enthalpy and entropy for base-pair opening, respectively, k is the Boltzmann constant, h is the Planck constant, and κ is the transmission coefficient of the activated state, which we assume to be 1 (*15*).

RESULTS

Assessment of Salt Effects. Although the basic exchange catalysts ammonia and TMA are uncharged, the high salt-content of the buffers originating from the acidic components leads to an inevitable increase of the ionic strength during the titrations. If the DNA helix does not preserve its structural and dynamic properties during the titration, the exchange data may be misinterpreted. To investigate the influence of the ionic strength on the structure of the DNA helix, CD spectra were recorded in the absence of added catalyst and at the buffer concentrations reached at the end of the titrations with ammonia and TMA. From Figure 1, it is observed that the CD spectrum of $d(CGCGAATTCGCG)_2$ changes in a small but significant way when ammonia is added while the spectrum is virtually unaffected by addition of TMA. These observations are paralleled in NOESY spectra acquired under similar conditions. Only very small chemical shift changes are induced by addition of TMA, while larger shifts, mainly of the sugar protons, are observed upon addition of ammonia to high concentrations (Supporting Information). Both buffers induce the largest resonance shifts for protons at the ends of the helix. The changes induced in the CD spectrum of $CGCA_8CGC/GCGT_8GCG$, by a high ammonia buffer concentration, are very similar to those observed for the 12-mer, suggesting that the spectral alterations reflect global and sequence-independent properties (data not shown).

The calculation of imino proton exchange times from eq 5 requires that the nonexchange contributions to the recovery rate are unaffected by large additions of catalyzing buffer. This is normally not the case, and the recovery times decrease when the ionic strength increases (*29*, *30*). To assess the magnitude of this effect, solutions of the NH_4Cl and $NH(CH_3)_3Cl$ salts with the pH adjusted to 4.6 and 6, respectively, were titrated to the 12-mer at 15 °C, and the recovery times were measured. Under these pH conditions, the base catalyst concentrations are negligible. Before addition of the salts, CD spectra were recorded and found to be identical to the spectra recorded at the higher pH values used in the titrations (data not shown). Furthermore, the recovery rates of the imino proton resonances were independent of the pH in this range. An exception was a slight decrease of some guanine

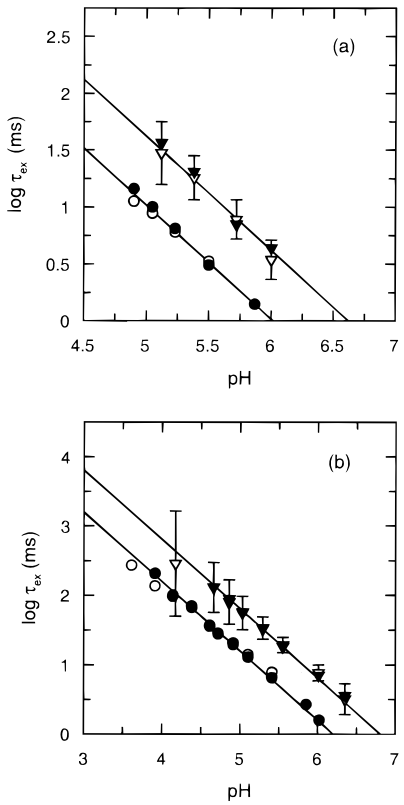

FIGURE 2: Exchange of the imino proton of (a) guanosine and (b) thymidine at 20 °C, catalyzed by ammonia (▽, ▼) or trimethylamine (○, ●). The mononucleoside and catalyst buffer concentration was 5.0 and 8.6 mM, respectively. The exchange times τ_{ex} were obtained both from inversion−recovery (▽, ○) and line-broadening (▼, ●) measurements. For one data set (▽) representative error bars are displayed. The linear fits to eq 2 are shown.

imino proton recovery rates at pH 4.6, consistent with initiation of acid catalysis (*31*). The recovery rates, that initially were in the range 0.36−0.37 s, had decreased with 15 and 24% at the end of the titrations with the NH_4Cl and $NH(CH_3)_3Cl$ salts, respectively. These changes were too small to significantly affect the evaluation of the exchange times and were not accounted for. These observations also ensure that potential salt effects on the exchange via OH^- ions and intrinsic catalysis (*25*) are negligible. On the other hand, for the 14-mer A-tract sequence, the recovery times decreased, roughly exponentially and independent of sequence position, by 47%, and the exchange times were corrected accordingly (Figure 7a).

Imino Proton Transfer from Mononucleosides. The imino proton exchange times of the mononucleosides thymidine and guanosine were determined at 20 °C in the presence of 8.6 mM ammonia or TMA buffer at several pH values in the range 3.5−6.5. The exchange times show a linear dependence on the pH with a slope equal to 1 as expected from eq 2 (Figure 2). The molar transfer rates shown in Table 1, derived from linear fits to eq 2, are in reasonable agreement with transfer rates previously obtained at 15 °C (*13*). Both for thymidine and guanosine, the transfer rates in the presence of TMA are approximately 0.8 times lower than in the presence of ammonia, which implies that the encounter complex forming efficiency of TMA is about half that of ammonia. Consequently, even though TMA has higher pK_a than ammonia, it is a somewhat less effective catalyst.

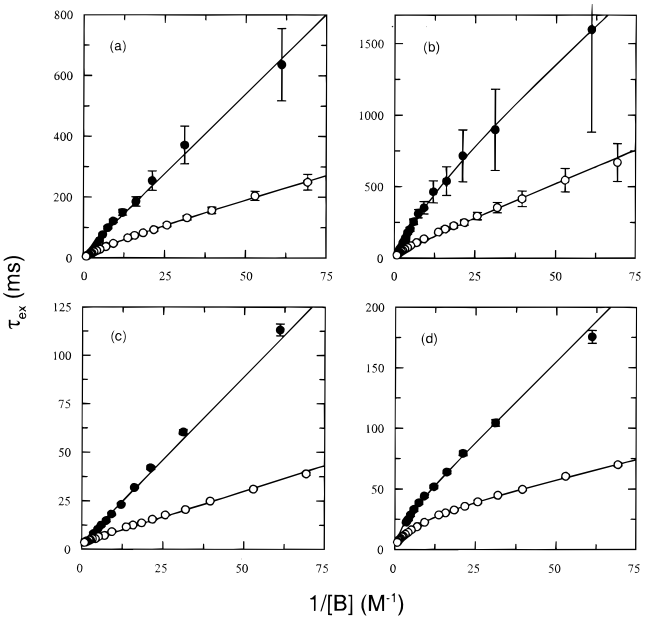

FIGURE 3: Imino proton exchange times τ_{ex} of the (a) CG3, (b) GC4, (c) AT5, and (d) AT6 base-pair of $d(CGCGAATTCGCG)_2$ displayed as a function of the inverse ammonia (○) and TMA (●) concentration at 20 °C and pH 9.5. Both data sets were simultaneously fitted to eq 3 ($n = 2$) with the exchange times weighted according to their errors, obtained by propagation of the standard deviations in the recovery times.

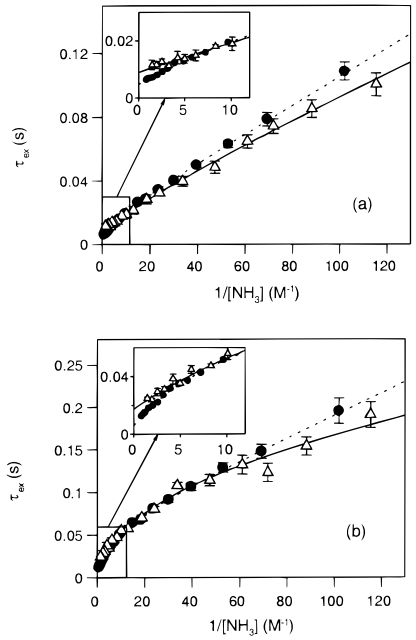

FIGURE 4: Imino proton exchange times τ_{ex} at 20 °C of the AT5 (a) and AT6 (b) base pairs of $d(CGCGAATTCGCG)_2$ catalyzed by ammonia at pH 9.5 (●) and 8.8 (△). The exchange data were fitted to eq 3 as described in the legend to Figure 3.

Neither the presence of 0.1 M NaCl in the solution nor the use of 2',3'-cyclic monophosphate nucleotides had any significant effect on the transfer rates measured. Furthermore, the temperature dependency of the transfer rates was small (data not shown).

Base-Pair Opening Kinetics. In the presence of increasing amounts of an exchange catalyst, the imino proton exchange time approaches the base-pair lifetime τ_{op}. How fast this limiting exchange time is reached depends on the base-pair dissociation constant K_d. However, several unknown factors,

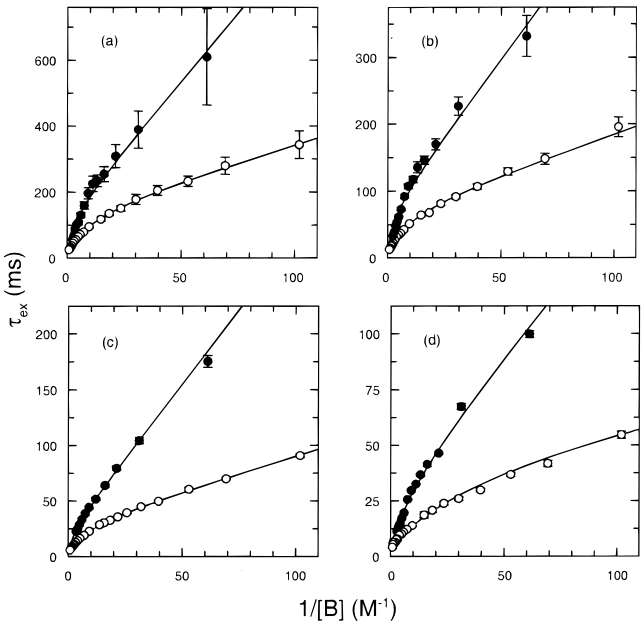

FIGURE 5: Imino proton exchange times τ_{ex} of the AT6 base pair in d(CGCGAATTCGCG)$_2$ at (a) 10 °C, (b) 15 °C, (c) 20 °C and (d) 25 °C, displayed as a function of the inverse ammonia (○) or TMA (●) concentration at pH 9.5. The exchange data were fitted to eq 3 as described in the legend to Figure 3.

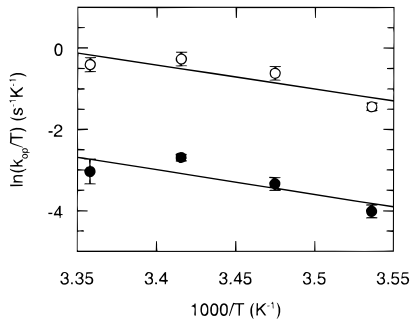

FIGURE 6: Eyring plots for the opening rates of the fast (○) and slow (●) opening mode of the AT6 base-pair in d(CGCGAATTCGCG)$_2$, obtained from the data in Table 3. The linear fits to eq 7 are shown. The fittings were performed with weighting of the exchange times according to their errors obtained by propagation of the standard deviations in the recovery times.

like steric hindrance and concentration activity effects, influence the frequency of encounters between the catalyst and the imino proton and, consequently, affect the receptivity of the imino proton for exchange catalysis. For this reason, it is convenient to introduce an apparent open-state lifetime $\alpha\tau_{cl}$ and apparent dissociation constant $\alpha k_{op}/k_{cl} = \alpha K_d$. For brevity, $\alpha\tau_{cl}$ and αK_d will be referred to as the open-state lifetime and the base-pair dissociation constant in the following, but with the understanding that these apparent quantities equal the real ones only if $\alpha = 1$.

Measurements of the imino proton exchange rates of d(CGCGAATTCGCG)$_2$ were carried out with ammonia and TMA as exchange catalysts at 10, 15, 20, and 25 °C. The pK_a of TMA is 9.80 at 25 °C and a high solution pH was necessary to achieve sufficient amount of base component in the buffer. At pH 9.5, no destabilization of the helix has occurred as judged from helix-melting measurements with UV spectroscopy (data not shown) and the CD spectrum is identical to the spectra recorded at lower pH (vide supra). Hence, this pH was chosen for comparative measurements

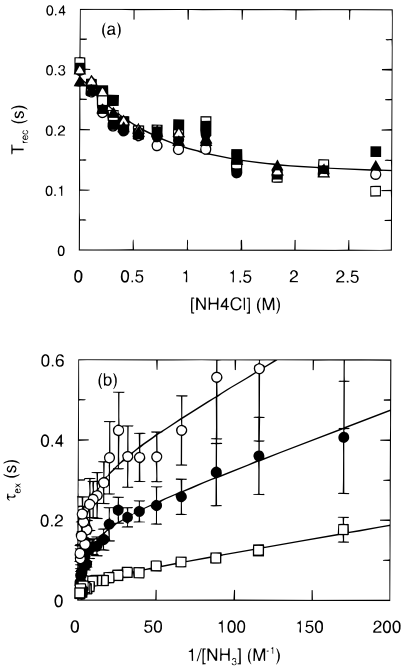

FIGURE 7: (a) The ammonium chloride salt dependence of the recovery times for T4 (▲), T5 (△), T6 (■), T7 (□), T8 (●), and T9/10/11 (○) in CGCA$_8$CGC/GCGT$_8$GCG at pH 4.6 and 20 °C. (b) Exchange times τ_{ex} of the imino proton of T5 (□), T6 (●), and T7 (○) at pH 8.8 and 20 °C displayed as a function of the inverse ammonia base concentration. The exchange data were fitted to eq 3 as described in the legend to Figure 3.

Table 1: Imino Proton Transfer Rates from the Isolated Mononucleosides at 20 °C, Obtained from Fitting of the Exchange Data to Equation 2

	transfer rate ($\times 10^8$ s^{-1} M^{-1})		
catalyst	TMA	NH_3	
guanosine	2.3 ± 0.4	2.9 ± 0.5	2.1[a]
thymidine	1.5 ± 0.3	1.9 ± 0.3	2.0[a]

[a] 15 °C (reference 13).

with ammonia. Some titrations with ammonia were also conducted at pH 8.8. The kinetics of the three outermost base pairs were not investigated since they are destabilized by "end-fraying" effects (*32*).

The exchange times of the four central base pairs are displayed as a function of the inverse ammonia and TMA concentrations in Figure 3. At high catalyst concentrations, the exchange times measured with both catalysts extrapolate toward the same *y*-axis intercept and therefore monitor the same openings (see Materials and Methods). However, the exchange times of the G3, G4, and T6 imino protons do not show a linear dependence on the inverse catalyst concentration over the whole concentration range. In the case of T6, the curvature is clearly larger than can be accounted for by errors in the data points. The linearity of the τ_{ex} vs 1/[B] plots relies on the assumptions of an opening/closing mechanism that protects the imino proton from exchange in the closed state and of the prevalence of a single open state. It is generally considered that exchange of a hydrogen-bonded proton only occurs when the hydrogen bond is broken (*8*). Furthermore, exchange from the closed state has not been detected even for the terminal base pairs in double helical DNA (*9*). Hence, the source of the nonlinearity is likely to be the presence of multiple open states. From eq 3, it is seen

Table 2: Kinetic Parameters of the Fast-Opening Mode for the Four Innermost Base Pairs of d(CGCGAATTCGCG)$_2$ Obtained from Ammonia and TMA Catalysis at 20 °C and pH 9.5 and, Only with Ammonia as Catalyst, at 15 °C and pH 8.8[a]

	G3	G4	T5	T6
		pH 9.5, 20 °C		
τ_{op} (ms)	<1	16 ± 6	3.4 ± 0.2	4.5 ± 0.8
$\alpha_{NH3}K_d$ ($\times 10^{-7}$)	5 ± 1	3.0 ± 0.7	99 ± 18	15 ± 4
$\alpha_{NH3}\tau_{cl}$ (ns)	<0.5	5 ± 3	34 ± 8	7 ± 3
$\alpha_{TMA}/\alpha_{NH3}$	0.51 ± 0.18	0.34 ± 0.17	0.39 ± 0.16	0.43 ± 0.23
		pH 8.8, 15 °C		
τ_{op} (ms)[b]	5 ± 2	34 ± 3	9 ± 0.4	23 ± 2
τ_{op} (ms)	<1	20 ± 2	9 ± 4	19 ± 7
$\alpha_{NH3}K_d$ ($\times 10^{-7}$)	5.6 ± 0.3	1.7 ± 0.2	43 ± 9	10 ± 1
$\alpha_{NH3}\tau_{cl}$ (ns)	<0.6	3.4 ± 0.7	39 ± 25	23 ± 9
τ_{op} (ms)[c]	4 ± 2	36 ± 3	8 ± 2	30 ± 2
$\alpha_{NH3}K_d$ ($\times 10^{-7}$)[c]	5.6	1.7	45	20
$\alpha_{NH3}\tau_{cl}$ (ns)[c]	2.2	6.1	36	60

[a] The base-pair lifetime τ_{op}, dissociation constants $\alpha_{NH3}K_d$, and open state lifetimes $\alpha_{NH3}\tau_{cl}$ are shown. At pH 9.5, also the accessibility ratios $\alpha_{TMA}/\alpha_{NH3}$ are given. The parameters at pH 9.5 were obtained by simultaneous fitting of the exchange times from the ammonia and TMA titrations to a two opening-modes model ($n = 2$ in eq 3), except for T5 where the linear eq 4 was used. At pH 8.8, the exchange times data were fitted to eq 3 with $n = 2$. The errors were propagated from the standard deviations in the recovery times. The intrinsic transfer rates given in Table 1 were used to calculate the dissociation constants at both temperatures. [b] Obtained from a linear fitting of the high concentration data in the range 0.05−0.7 M. For T5 and T6 the titration data at pH 8.8 is shown in Figure 4. [c] Reference *12*.

that the τ_{ex} vs 1/[B] plots will be nonlinear if open states with different values of k_{cl}/α exist. The two data sets in Figure 3 were simultaneously fitted to eq 3 with two open states ($n = 2$), except the linear exchange data of T5 that were fitted to eq 4. The exchange data obtained with the two catalysts are consistent with common opening rates but a catalyst-dependent accessibility affecting the apparent dissociation constants. Thus, for AT6 the base-pair opening event produces two open states differing in the k_{cl}/α property. As will be discussed later, quantification for AT6 shows that the opening rates to the two states differ by a factor of 13−15. The two opening modes will be referred to as a fast and a slow component of the total opening.

The kinetic parameters and the relative accessibility of the two catalysts, obtained from the fits in Figure 3, are shown in Table 2. In addition, Table 2 contains kinetic parameters derived from an ammonia titration carried out at 15 °C and pH 8.8 to enable comparison with previous results obtained under these conditions (*12*). The general trend in Table 2, although most pronounced for the AT base pairs, is a decrease of the lifetimes and an increase of the dissociation constant at the higher pH and temperature. By comparison of Table 2 with the data at 15 °C in Table 3 and inspection of Figure 4, it is clear that the lifetimes decrease more than what can be accounted for by the raise in temperature. When the pH increases from 8.8 to 9.5, the extrapolated lifetime changes from 19 to 6.4 ms and from 9 to 5.5 ms for the AT6 and AT5 base pair, respectively. Increasing the temperature to 20 °C gives a further decrease of the lifetime to 4.5 ms for AT6 and to 3.4 ms for AT5 (Table 2). The exchange data of T5 and T6 at 15 °C obtained from titrations with ammonia buffers at pH 8.8 and 9.5 are shown overlaid in Figure 4. Although the two data sets yield somewhat different lifetimes (vide supra), a close similarity in the exchange behavior is evident. Most importantly, the strong curvature observed for AT6 is identical. The exchange data are also in very good agreement with previous results that invariably have utilized eq 4 to interpret imino proton exchange in kinetic terms. A linear fit in the high concentration range 0.05−0.7 M of the titration at pH 8.8 yields base-pair lifetimes and dissociation constants virtually identical to previous results (Table 2). The only exception is the somewhat shorter lifetime of 23 ms for AT6 in the present study compared to 30 ms obtained by Guéron and Leroy (*12*). However, it should be noted that the agreement in the obtained dissociation constants partly is circumstantial since the present study has used slightly different values of the transfer rates from the mononucleosides (cf. Table 1). It is likely that an incompatibility in the estimate of the base concentration of the buffers used in the two studies has compensated for this difference. From Table 2, it is also observed that for all four central base pairs of the 12-mer the accessibility is reduced for TMA compared to ammonia by a similar factor of 2−3, although the dissociation constants differ by 2 orders of magnitude.

For the AT6 base pair, a detailed analysis is possible also of the slow opening mode. In Figure 5, the exchange data from ammonia and TMA titrations carried out at 10, 15, 20, and 25 °C are shown, and the kinetic parameters derived from a simultaneous fitting of the two data sets to eq 3 with two opening modes are given in Table 3. The titrations with ammonia and TMA are compatible with the same, mutually different, opening rates to the two open states. The fast-mode lifetimes are in the range 5−15 ms while the slow-mode lifetimes are in the range 50−200 ms. The longer lifetimes for the slow opening mode taken together with the dissociation constants being 3−6 times higher yield open-state lifetimes more than 2 orders of magnitude longer than for the fast mode (Table 3). For example, at 10 °C, the lifetimes are 15 and 196 ms and the dissociation constants are 3.4×10^{-7} and 21×10^{-7}, for the fast and slow opening mode, respectively. In this case, lower limits ($\alpha = 1$) for the lifetimes of the open states reached by the fast and slow opening modes are 5 ns and 0.4 μs, respectively. In general, the open-state lifetimes are in the nanosecond region for the fast opening mode and close to 1 μs for the slow mode (Tables 2 and 3). However, a prolongation of the open-state lifetimes is associated with increasing the temperature. The lifetimes of the open states corresponding to the fast and slow opening mode change from 5 to 25 ns and from 0.4 to 1 μs, respectively, when the temperature is raised from 10 to 25 °C. The catalyst accessibility ratios $\alpha_{TMA}/\alpha_{NH3}$ are, on the other hand, independent of the temperature in the range used in the experiments, although different for the two open states, about 0.4 for the fast mode and 0.3 for the slow mode (Table 3). By comparing Tables 2 and 3, it is seen that the variation in the accessibility ratio at different temperatures is much smaller than between different base pairs.

In Figure 6 the opening rates obtained from the fits in Figure 5 are shown as a function of the temperature in an Eyring plot. By fitting to eq 7, the activation energy was found to be 59 kJ/mol for the fast mode and 66 kJ/mol for the slow mode. The activation enthalpy is about 50 kJ/mol for both modes, and the difference in activation energy between the two modes is accounted for by higher activation entropy for the slow mode.

Table 3: Kinetic Parameters for the Two Opening Modes of the AT6 Base Pair in d(CGCGAATTCGCG)$_2$ at pH 9.5 and Different Temperatures[a]

	10 °C	15 °C	20 °C	25 °C
		Fast Mode		
τ_{op} (ms)	14.9 ± 1.4	6.4 ± 1	4.5 ± 0.8	5.1 ± 0.9
$\alpha_{NH3}K_d$ ($\times 10^{-7}$)	3.4 ± 0.6	5.9 ± 1	15 ± 4	48 ± 16
$\alpha_{NH3}\tau_{cl}$ (ns)	5.1 ± 1.4	3.8 ± 1.2	6.8 ± 3	25 ± 13
$\alpha_{TMA}/\alpha_{NH3}$[b]	0.41 ± 0.24	0.36 ± 0.20	0.43 ± 0.23	0.35 ± 0.24
		Slow Mode		
τ_{op} (ms)	196 ± 31	98 ± 15	51 ± 4	70 ± 22
$\alpha_{NH3}K_d$ ($\times 10^{-7}$)	21 ± 5	37 ± 7	70 ± 26	144 ± 86
$\alpha_{NH3}\tau_{cl}$ (μs)	0.4 ± 0.2	0.4 ± 0.1	0.4 ± 0.2	1.0 ± 0.9
$\alpha_{TMA}/\alpha_{NH3}$[b]	0.32 ± 0.18	0.33 ± 0.15	0.28 ± 0.11	0.29 ± 0.16

[a] The inverse opening rates τ_{op}, dissociation constants αK_d, open state lifetime $\alpha_{NH3}\tau_{cl}$, and accessibility ratios $\alpha_{TMA}/\alpha_{NH3}$ are shown. The parameters were obtained by simultaneous fitting of the exchange times from the ammonia and TMA titrations to a two opening-modes model ($n = 2$ in eq 3). Errors were propagated from the standard deviations in the recovery times. The intrinsic transfer rates given in Table 1 were used to calculate the dissociation constants neglecting temperature effects. [b] The relatively large errors in the accessibility ratios originates from the errors in the intrinsic imino proton-transfer rates from the mononucleosides.

Table 4: Kinetic Parameters of the Two Opening Modes for the Central A-Tract of CGCA$_8$CGC/GCGT$_8$GCG at pH 8.8 and 20 °C Obtained from Titration with Ammonia[a]

	T5	T6	T7	T8	T9−11
		Fast Mode			
τ_{op} (ms)	<30	<30	<100	<200	<60
$\alpha_{NH3}K_d$ ($\times 10^{-7}$)	5.3 ± 2.1	1.5 ± 0.4	0.6 ± 0.3	0.5 ± 0.4	2.7 ± 1.2
		Slow Mode			
τ_{op} (ms)	60 ± 10	210 ± 30	340 ± 80	310 ± 80	220 ± 60
$\alpha_{NH3}K_d$ ($\times 10^{-7}$)	72.1 ± 2.1	34.7 ± 1.4	22.6 ± 1.5	11.9 ± 0.5	17.8 ± 0.9
$\alpha_{NH3}\tau_{cl}$ (μs)	0.4 ± 0.1	0.7 ± 0.1	0.8 ± 0.1	0.4 ± 0.1	0.4 ± 0.1

[a] The inverse opening rates τ_{op} and the dissociation constants αK_d are shown for both modes. For the slow mode, also the open state lifetimes $\alpha_{NH3}\tau_{cl}$ are given. The parameters were obtained by fitting the exchange times to a two opening-modes model (n=2 in eq 3). Errors were propagated from the standard deviations in the recovery times. The intrinsic transfer rate given in Table 1 was used to calculate the dissociation constants.

Since the curvature is most pronounced for the central AT base pair of d(CGCGAATTCGCG)$_2$, the base-pair dynamics was studied also in the 14-mer CGCA$_8$CGC/GCGT$_8$GCG to find out whether the curvature in the exchange data is related to the known anomalous properties of A-tract sequences (*33*). In Figure 7b, the titration data with ammonia as catalyst are shown for the AT5, AT6, and AT7 base pairs. It is clear that the curvature becomes progressively stronger toward the center of the oligomer. The base-pair lifetimes and the dissociation constants evaluated from eq 3 with two open states are shown in Table 4. As previously observed (*14*, *34*) the 5′-end of the tract is more labile with higher dissociation constants and shorter lifetimes than base pairs at the 3′-end (Table 4). This observation is valid for both modes. The lifetimes of the slow mode are more than 300 ms for the central AT-base pairs and are among the longest observed in any DNA double helices. However, these lifetimes are not the same as the base-pair lifetimes that rather are the inverse of the sum of the opening rates to both open states. The lifetimes of the fast mode could not be accurately determined due to the strong curvature that makes the *y*-axis intercepts uncertain. However, the lifetimes of the fast mode are at least a factor of 2−5 shorter than the corresponding lifetimes of the slow mode. As shown in Table 4, the central base pairs of the A-tract sequence also exhibit open-state lifetimes of the slow opening mode close to 1 μs.

In summary, the base-pair opening in the central A-tract of both oligomers resolves into one frequently occurring component with a low dissociation constant and another less likely component with a higher dissociation constant.

DISCUSSION

The most outstanding feature of the present study is the curvature observed in the τ_{ex} vs 1/[B] plots (Figure 3, 4, 5, and 7). Nonlinearities in these types of plots have not previously been reported, and it is natural to ask whether the curvature reflects kinetics or has another origin. For example, a salt-induced conversion of the DNA helix to a different structural species, that exhibits altered base-pair dynamics, would produce curvature. However, CD spectra and 2D-NMR experiments show no indications of significant salt effects on the structure (Figure 1 and Supporting Information). Almost no spectral alterations are discernible by addition of the TMA buffer, while significant, but modest, effects are observed in the presence of high concentrations of the ammonia buffer. Both catalysts produce, however, exchange times with closely analogous curvature consistent with the same base-pair lifetimes. It is seen from Figure 3 that at 20 °C a curvature is present in the exchange data of T6 with both catalysts while the T5 exchange data are linear in both cases (Figure 3, panels c and d). Hence, the curvature is caused by a property intrinsic to the AT6 base pair. Particularly strong evidence that salt effects do not cause the curvature is provided by Figure 4 where the exchange data are shown to produce very similar curvatures and largely overlap at pH 8.8 and 9.5, although the salt concentrations are 2.5 times higher in the titration at the lower pH. Another possible source of curvature, unrelated to exchange kinetics, is a decrease in the longitudinal relaxation contribution to the recovery rates of the imino protons, most likely induced by the increased ionic strength in the course of the titration. Again Figure 4 indicates that salt effects are unlikely to cause

curvature in this fashion. In addition, titrations were performed at low pH to assess the effect of the salts on the longitudinal relaxation. Indeed, an effect was observed in accordance with previous investigations (*29*, *30*). The salt-induced decrease of recovery rates was, however, too small to significantly affect the evaluation of the exchange times and did not affect the curvature at all (data not shown). For example, at pH 4.6, the recovery rate of T6 decreased by 15% at the ammonium chloride concentration reached at the end of the catalyst titrations. On the other hand, at pH 8.8, the recovery rate of T6 decreases by almost a factor of 20 and, consequently, the decrease of the longitudinal relaxation is negligible in comparison. It should also be noted that the present data is consistent with previous measurements carried out in the high-concentration regime (*12*) (see Table 2). The novel features are, in fact, observed in the low to intermediate concentration region where the salt effects are smaller. Hence, all evidence indicates that the curvature in the τ_{ex} vs 1/[B] plots reflects exchange kinetics.

In terms of base-pair opening kinetics, the existence of two open states with different lifetimes $\alpha\tau_{cl}$ is the most straightforward explanation of the curvature observed in the exchange data of the AT6 base pair. For instance, the curvature at 15 °C (Figure 5b) is consistent with the imino proton exchange occurring from a short-lived open state formed with a high rate of 160 s^{-1} exhibiting a lifetime $\alpha\tau_{cl}$ in the nanosecond range and from a more long-lived open state with a lifetime $\alpha\tau_{cl}$ close to 1 μs formed with a lower rate of 10 s^{-1}. Many qualitative arguments have favored a value for α close to 1 for the small uncharged catalyst ammonia (*1*, *12*, *13*). For terminal base pairs, a more quantitative estimate of 0.37−0.92 has been derived (*9*). Hence, it is likely that the apparent open-state lifetimes reflect the true ones at least within an order of magnitude. For the uncharged catalysts used in the present study, α is expected to be less than 1 and the quantities $\alpha_{NH3}\tau_{cl}$ are lower limits of the true open-state lifetimes. However, it should be noted that if the accessibility of the imino proton is strongly reduced in the open state formed by the fast opening mode, a situation at variance with current belief (vide supra), the lifetime may be in the microsecond range also for the open states of the fast opening mode.

The kinetics of the frequently occurring opening (the fast mode) of the present study is almost identical to that obtained by previous investigators that has assumed a single open state (Table 2). This is expected since the emphasis in earlier studies has been to reach as high catalyst concentration as possible to achieve maximum accuracy in the extrapolations (*12*). However, the slow mode reveals itself mainly in the low-intermediate concentration range. Under most circumstances, the catalytic receptivity of the base-paired imino proton is weak, and the error in the exchange time as derived from the difference in eq 5 is large unless the concentration of catalyst is high (cf. Figure 2, panels b and d). In contrast, the AT6 base-pair exhibits strongly increased exchange rates already at relatively low catalyst concentration due to the long open-state lifetime of the slow opening mode. Also the CG3 and GC4 base-pairs appear to exhibit some curvature in Figure 2. The larger errors in the exchange data at low concentration make it difficult to establish the existence of a secondary opening mode for these two base pairs unambiguously. In any case, either the dissociation constant or the rate of formation of the open state must be lower than for the corresponding slow opening mode of AT6.

Measurements by Moe and Russu (*35*) yielded considerably longer lifetimes for the central four base pairs of $d(CGCGAATTCGCG)_2$ than subsequently found by Guéron and Leroy (*12*). Noting that both investigations assumed eq 4 to be valid and that Moe and Russu used lower ammonia concentration, the discrepancy may be explained by the curvature making the extrapolated lifetimes dependent on the catalyst concentration range. Furthermore, it was recently found that different extrapolated lifetimes are obtained with ammonia and TMA as exchange catalysts (*15*). That observation is rendered unlikely by the present study. It seems plausible that the lower concentration of TMA, due to its higher pK_a, in combination with curvature caused the difference in extrapolated lifetimes. It is also noteworthy that the pH dependence of the base-pair lifetimes evident in Figure 4 indicates that the lifetimes obtained under the basic conditions of the exchange catalyst titrations may underestimate the base-pair lifetimes prevailing under physiological conditions.

The activation energies 59 and 66 kJ/mol for the fast and slow opening mode, respectively, fall between 50 kJ/mol measured for the central AT base pair of $d(CGCGATCGCG)_2$ and 96 kJ/mol obtained for A_{14}/T_{14} (*14*). The temperature dependence of both opening rates is very similar, yielding an activation enthalpy of about 50 kJ/mol. This indicates that the base-pair disruption event could be the same for both opening modes. To explain the observed kinetics, the conformational space sampled by the DNA helix should normally favor the formation of open states characterized by lifetimes in the nanosecond range but also, although less frequently, open states with a lifetime of about 1 microsecond is permitted.

A comparison of the catalytic efficiency of ammonia and TMA gives information about their relative accessibilities to the open states and may yield information regarding the open states themselves. From the accessibility ratios listed in Tables 2 and 3, the variation between different base pairs is observed to be larger than for the same base pair at different temperatures. Hence, the accessibility ratio appears to reflect sequence dependent properties. Steric hindrance in the open state as well as the difference in diffusion coefficient of the larger oligomer and the mononucleoside affects the parameter α. However, from the form of eq 3, it is evident that activity effects on the base concentration also will enter into the parameter α. Recently, it was demonstrated that ammonium ions bind in the minor groove of DNA, in particular, to the narrow minor groove of A-tract sequences (*36*). From Figure 4, it is concluded that the curvature is nearly independent of the ammonium ion concentration in the range used in the titrations. Consequently, any effect of ion binding must saturate at relatively low concentration. Ammonium ion binding could, however, lead to a higher effective ammonia concentration in the groove than in the bulk solution if the ammonium ions are in equilibrium with their ammonia base counterpart. The specificity of ammonium ion binding to A-tracts was attributed to a good fit of the ion in the narrow groove (*36*). Hence, the bulkier TMA ion is not expected to bind in a similar fashion and the ratios $\alpha_{TMA}/\alpha_{NH3}$ should decrease by activity effects. Thus, the similarity in the curvature in the exchange data from the

titrations with ammonia and TMA also indicates that the curvature is unrelated to ammonium ion binding. The accessibility ratio is 0.4 for the open state of the fast opening mode and 0.3 for the slow mode, independent of the temperature in the range 10−25 °C. This consistent difference indicates that the two open states are distinct.

From Tables 2 and 4, it is observed that the lifetimes for both modes (i.e., the inverse of the opening rates to the two open states) increase toward the center of the A_2T_2 and A_8/T_8 tracts, in agreement with previous investigations (*14*, *34*). From Figures 3 and 7, it is, however, also clear that the curvature increases from the 5′-end toward the 3′-end of the A-tract. Since it is known that the A-tract narrows in the same direction (*24*), the degree of curvature in the exchange data appears to be connected to the narrowness of the minor groove. It is thus tempting to, at least in part, assign the curvature to an accessibility effect. If the fast mode corresponds to the thymine base being accessed by the catalyst in the minor groove, narrowing the minor groove may lead to a decrease of the apparent dissociation constant for the fast mode and an enhanced curvature would result. The apparent open-state lifetimes of the slow mode are independent of the position in the A-tract and similar in the two oligomers (Table 4), indicating that the accessibility is invariable in this case. The wider and more accessible major groove is a tentative candidate for this open state.

CONCLUSIONS

It has been shown that at least two distinct open states exist for the central AT base pair of $d(CGCGAATTCGCG)_2$. In addition to the previously known open state with a lifetime of about 5 ns at 20 °C, a long-lived open state with a lifetime close to 1 μs has been discovered. Conservatively, these estimates should be considered as lower limits of the lifetimes since they rely on the assumption of a similar imino proton accessibility in the open states and in the mononucleoside. The rate of formation of the short-lived open states is in accordance with previous measurements while the long-lived open state is formed 10−15 times less frequently. Hence, previous estimates of the base-pair lifetimes are not affected by these results. Furthermore, the long-lived open states are also present in the interior of the A-tract $CGCA_8CGC$/$GCGT_8GCG$ and may be connected to the known anomalous properties of A-tract DNA.

The present finding of spontaneous base-pair disruptions that leaves the bases unpaired for longer times than previously appreciated may be of relevance for sequence specific DNA recognition by proteins, interactions with ligand, and DNA damage.

SUPPORTING INFORMATION AVAILABLE

Expansions of the H6/H8−H1′ cross-peak region from NOESY spectra of $d(CGCGAATTCGCG)_2$ in the absence or presence of either TMA or ammonia buffer at concentrations similar to those reached at the end of the catalyst titrations. A scheme that shows the NOESY pulse sequence used for simultaneous suppression of the water and TMA proton signals. This material is available free of charge via the Internet at http://pubs.acs.org.

REFERENCES

1. Guéron, M., and Leroy, J. L. (1992) *Nucleic Acids Mol. Biol. 6*, 1−22.
2. Steitz, T. A. (1990) *Q. Rev. Biophys. 23*, 205−280.
3. Rozenberg, H., Rabinovich, D., Frolow, F., Hegde, R. S., and Shakked, Z. (1998) *Proc. Natl. Acad. Sci. U.S.A. 95*, 15194−15199.
4. Olson, W. K., Gorin, A. A., Lu, X. J., Hock, L. M., and Zhurkin, V. B. (1998) *Proc. Natl. Acad. Sci. U.S.A. 95*, 11163−11168.
5. Klimasauskas, S., Kumar, S., Roberts, R. J., and Cheng, X. (1994) *Cell 76*, 357−369.
6. Reinisch, K. M., Chen, L., Verdine, G. L., and Lipscomb, W. N. (1995) *Cell 82*, 143−153.
7. Dornberger, U., Leijon, M., and Fritzsche, H. (1999) *J. Biol. Chem. 274*, 6957−6962.
8. Englander, S. W., and Kallenbach, N. R. (1983) *Q. Rev. Biophys. 16*, 521−655.
9. Nonin, S., Leroy, J. L., and Gueron, M. (1995) *Biochemistry 34*, 10652−10659.
10. Teitelbaum, H., and Englander, S. W. (1975) *J. Mol. Biol. 92*, 55−78.
11. Teitelbaum, H., and Englander, S. W. (1975) *J. Mol. Biol. 92*, 79−92.
12. Guéron, M., and Leroy, J. L. (1995) *Methods Enzymol. 261*, 383−413.
13. Guéron, M., Charretier, E., Hagerhorst, J., Kochoyan, M., Leroy, J. L., and Moraillon, A. (1990) *Struct. Methods 3*, 113−137.
14. Leroy, J. L., Charretier, E., Kochoyan, M., and Guéron, M. (1988) *Biochemistry 27*, 8894−8898.
15. Leijon, M., Sehlstedt, U., Nielsen, P. E., and Gräslund, A. (1997) *J. Mol. Biol. 271*, 438−455.
16. Leroy, J. L., Gao, X. L., Guéron, M., and Patel, D. J. (1991) *Biochemistry 30*, 5653−5661.
17. Leroy, J. L., Gao, X. L., Misra, V., Guéron, M., and Patel, D. J. (1992) *Biochemistry 31*, 1407−1415.
18. Hvidt, A., and Nielsen, S. O. (1966) *Adv. Protein Chem. 21*, 287−386.
19. MacInnes, D. A. (1939) in *The principles of electrochemistry*, Reinhold Publishing, New York.
20. Perrin, D. D., and Dempsey, B. (1979) *Buffers For pH and Metal Ion Control*, p 162, Chapman & Hall, London.
21. Eigen, M. (1964) *Angew. Chem., Int. Ed. Engl. 3*, 1−72.
22. Patel, D. J., Pardi, A., and Itakura, K. (1982) *Science 216*, 581−590.
23. Plateau, P., and Guéron, M. (1982) *J. Am. Chem. Soc. 104*, 7310−7311.
24. Nadeau, J. G., and Crothers, D. M. (1989) *Proc. Natl. Acad. Sci. U.S.A. 86*, 2622−2626.
25. Guéron, M., Kochoyan, M., and Leroy, J. L. (1987) *Nature 328*, 89−92.
26. Geen, H., and Freeman, R. (1991) *J. Magn. Reson. 93*, 93−141.
27. Bauer, C., Freeman, R., Frenkiel, T., Keeler, J., and Shaka, A. J. (1984) *J. Magn. Reson. 58*, 442−457.
28. Glasstone, S., Laider, K. J., and Eyring, H. (1941) in *The Theory of Rate Processes*, McGraw-Hill, New York.
29. Folta-Stogniew, E., and Russu, I. M. (1996) *Biochemistry 35*, 8439−8449.
30. Leijon, M., and Leroy, J. L. (1997) *Biochimie 79*, 775−779.
31. Nonin, S., Leroy, J. L., and Guéron, M. (1996) *Nucleic Acids Res. 24*, 586−595.
32. Leijon, M., and Gräslund, A. (1992) *Nucleic Acids Res. 20*, 5339−5343.
33. Crothers, D. M., Haran, T. E., and Nadeau, J. G. (1990) *J. Biol. Chem. 265*, 7093−7096.
34. Moe, J. G., and Russu, I. M. (1990) *Nucleic Acids Res. 18*, 821−827.
35. Moe, J. G., and Russu, I. M. (1992) *Biochemistry 31*, 8421−8428.
36. Hud, N. V., Sklenar, V., and Feigon, J. (1999) *J. Mol. Biol. 286*, 651−660.

BI991863B